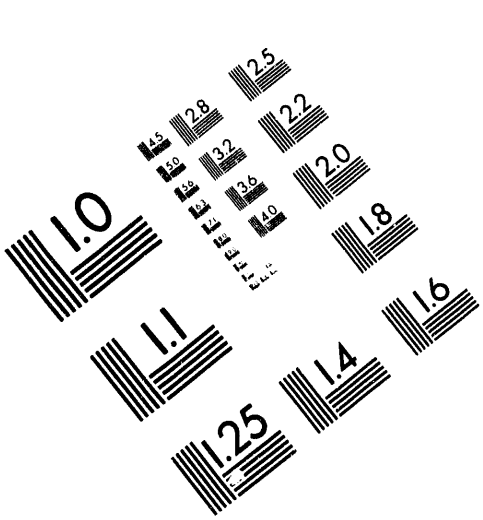

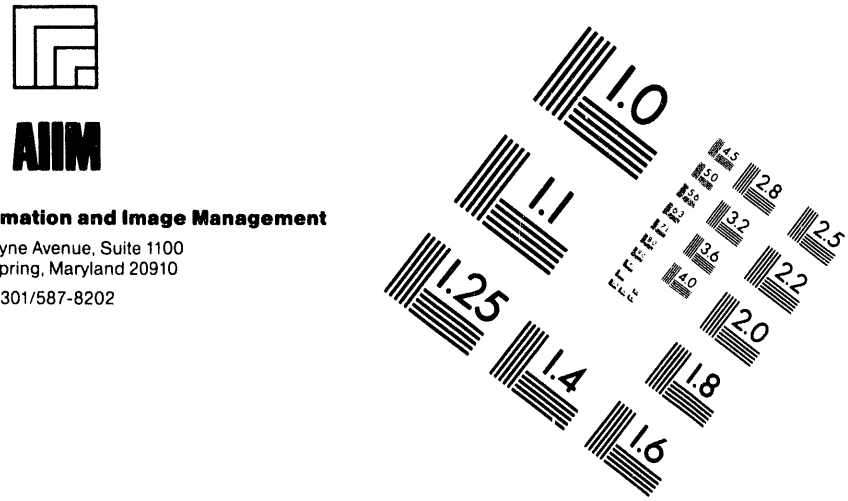

AIIM

Association for Information and Image Management
1100 Wayne Avenue, Suite 1100
Silver Spring, Maryland 20910
301/587-8202

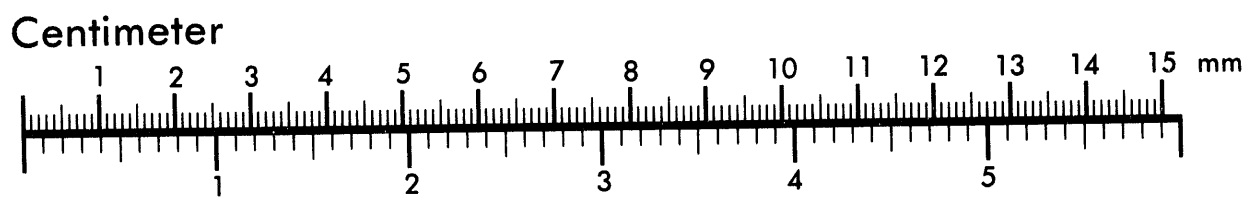

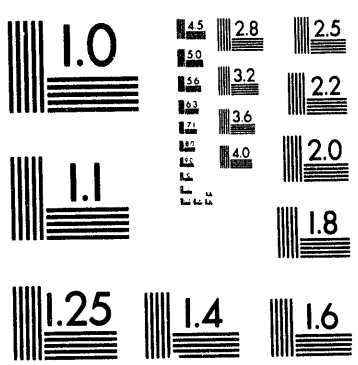

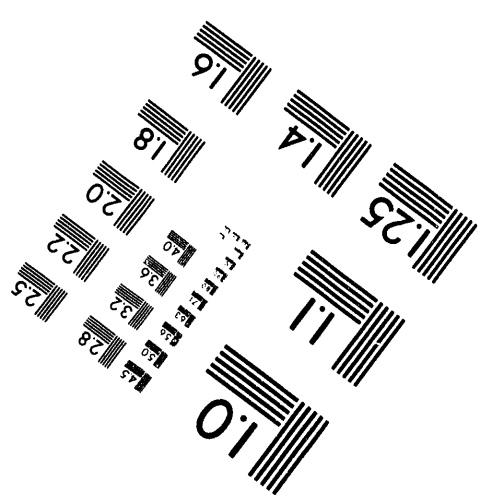

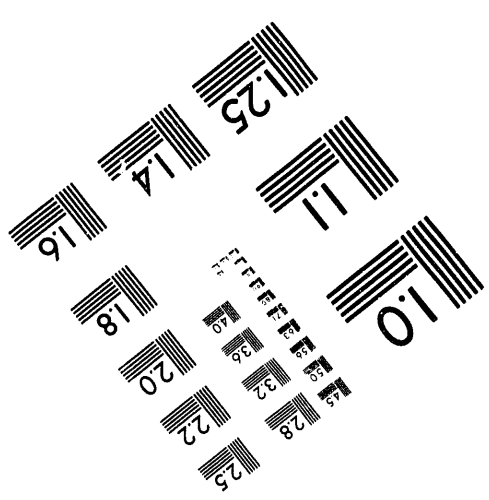

MANUFACTURED TO AIIM STANDARDS
BY APPLIED IMAGE, INC.

1 of 1

SAN094-2159C
Conf-940723--26

Stop Motion Microphotography of Laser Driven Plates

Alan M. Frank
Lawrence Livermore National Laboratory

Wayne M. Trott
Sandia National Laboratories

Laser driven plates have been used for several years for high velocity shock wave and impact studies[1,2,3,4,5]. Recent questions about the integrity and ablation rates of these plates coupled with an improved capability for microscopic stop motion photography led to this study.

For these experiments, the plates were aluminum, coated on the ends of optical fibers[6] . A high power laser pulse in the fiber ionizes the aluminum at the fiber/coating interface. The plasma thus created accelerates the remaining aluminum to high velocities, several kilometers per second. We defined 'thick' or 'thin' coatings as those where a flying plate (flyer) was launched vs. the material being completely ionized. Here we were specifically interested in the thick/thin boundary to develop data for the numerical models attempting to predict flyer behavior[7, 8].

Experimental Apparatus

The experimental apparatus of the flyer launcher (Figure 1) includes a single pulse Cr:Nd:GSGG drive laser (Allied Signal). The entire flyer launching apparatus was assembled at the Sandia National Laboratories in Albuquerque and transported to Livermore for these experiments. The laser has a 12ns pulse width and greater than 100mJ output. To maintain constant pulse width and mode, the laser is operated under constant drive and timing conditions. Variations in energy are accomplished with neutral density filters. The output of the laser is focused onto the larger end of a 2 meter long optical fiber which tapers from 1000μm to 400μm diameter. The purpose of the taper is both to reduce the energy density at the input surface, limiting the potential for damage, and also to help uniformly fill the fiber transmission modes. From the taper the energy is proximity coupled to the coated 400μm diameter fiber pigtail. An uncoated pigtail (or the coated pigtail after the coating has been blown off) is directed into a calorimeter to measure the actual system throughput and calibrate a splitter coupled calorimeter. Fiber filling and transmission modes[9] are also examined through an uncoated pigtail using a microscope objective coupled to CCD based beam profiler.

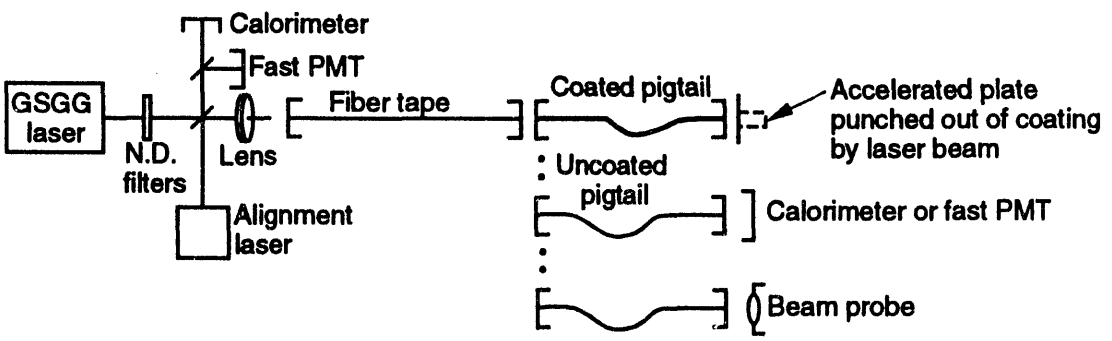

Figure 1. Schematic diagram of laser driven flyer launching apparatus.

The Micro Detonics Facility (μDF) was used to dynamically examine the flyers at or near the launch or 'jump off' time. The facility was established at Lawrence Livermore National Laboratory for small and micro scale studies of detonation and shock wave phenomena. The technology and apparatus of the facility grew out of Larry Shaw's work with fast gated intensified cameras[10] and one of the author's work in high speed microscopy[11, 12].

The diagnostic systems included the frame camera with a 75mm proximity focused photodiode intensifier for both reflective photography and back lit shadowgraph. The streak camera and the streak spectrometer were also used. The frame and streak cameras examine the same location on the target viewing through a common objective. The spectrometer is coupled to the experiment via an optical fiber, viewing a region perpendicular to the camera's line of sight. Illumination for the frame camera is provided by a pulsed broad band dye laser and for the streak camera by a continuous wave argon laser. Both lasers are combined to a single coaxial beam. The dye laser is focused to a circular region matching the field of view of the frame camera . Whereas, the argon is focused to a line matching the entrance slit of the streak camera. An overview of the facility is given in (Figure 2). For these experiments the explosives containment chamber is not used.

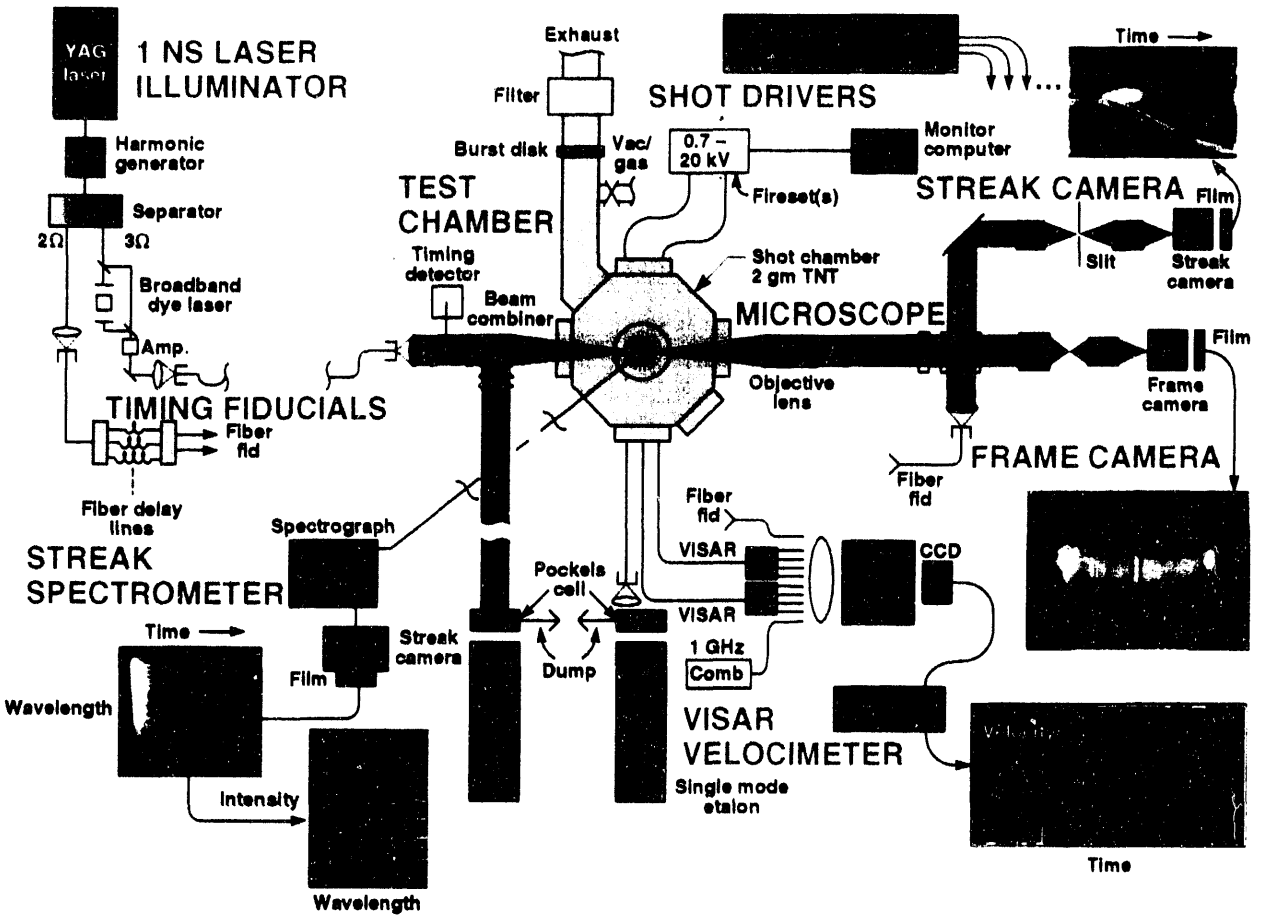

Figure 2. The Micro Detonics Facility

The key element of the system is the microscope. This is comprised of a combination of commercially available photographic lenses. Fast photographic objectives used backwards in conjunction with a long focal length lens, result in a diffraction limited, long working distance microscope. Diffraction limited performance is attained only when all lenses are used at their design conjugates, relay elements are used within their resolution limits, aberration creating elements are minimized and the system is well aligned. Then the resolution limits of the system are the diffraction of the objective and the spatial frequency response of the intensifier and streak tubes. The magnifications to the frame and streak cameras are separately adjustable by magnifying relays after images are split. The ideal magnification matches the objective limit to the tube response. At lower magnifications resolution is lost. At higher magnifications no additional resolution is realized; instead both depth of focus and field of view are lost. Magnifications from the object to the film plane for these experiments were 10X for the streak camera and 24X for the frame camera. Resolution was about 2μm over a 1.5mm field of view. Film (TMAX-400) was used as the recording medium for all cameras.

The streak spectrometer views only one point or integrated region in space dispersing the light in both spectrum and time. The region in this experiment is defined by the .22 numerical aperture of the fiber coupling the experiment to the spectrometer. The end of the cleaved 100μm silica fiber, was held about 1mm from the experiment thus defining the viewing region to about a mm diameter encompassing the entire experimental region. Two separate imaging configurations were used, near specular reflection (Figure 3a) and back lit shadowgraph (Figure 3b). In shadowgraph, the illumination light, fiber coupled from the laser, is aimed directly into the objective lens. It is refocused to a point before the target so that the expanding beam both fills the field of view at the target and the acceptance cone of the objective as defined by its numerical aperture. This last condition is essential to realize the full resolution of the microscope.

Fig 3. Experimental Configurations

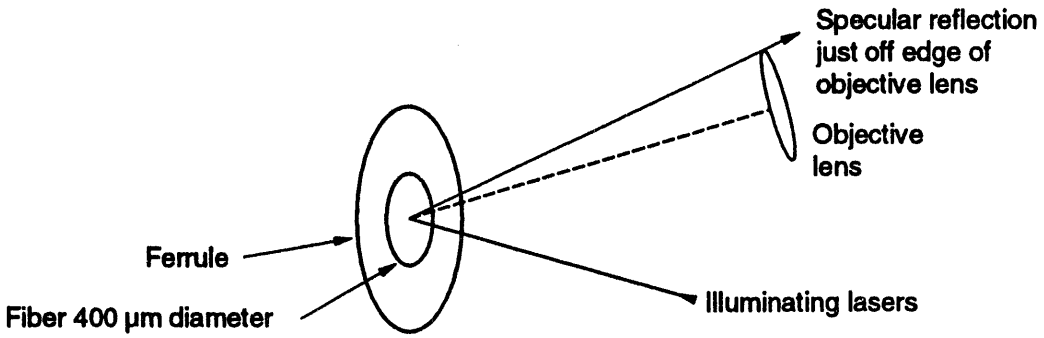

Figure 3a. Near Specular

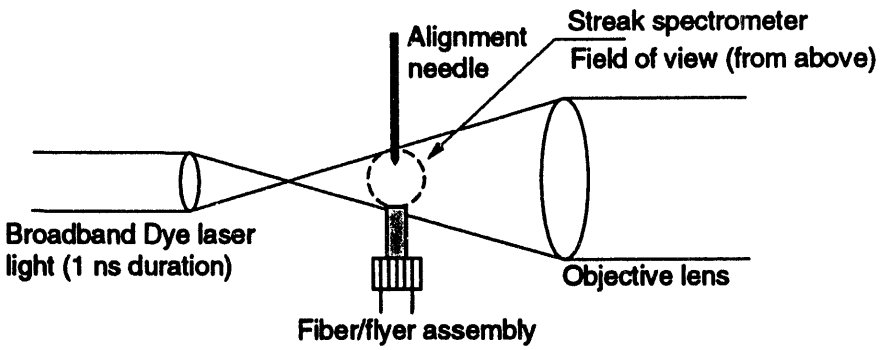

Figure 3b. Shadowgraph (with streak Spectrometer)

The aluminum flyer, vacuum deposited on a polished fiber, is a specularly reflecting mirror surface. However, no surface is perfectly specular and a diffuse component is always present. Some light is reflected at angles other than specular and there is a strong gradient of the amount of light reflected as the angle away from the specular increases. Additionally there is an aperture function. As the light incident on the target is not collimated, light at the objective fills a cone with a strong radial gradient. Thus if the surface is viewed at an angle such that the specular component of the illumination beam falls just outside the aperture of the objective, then small angular perturbations on the surface will reflect significantly more or less light into the objective. The result is a high contrast image where extremely small perturbations are highly visible.

Two versions of the near specular configuration were used. Both arrangements used a 110mm F/2.0 objective with a 70mm working distance. Interference between the 50mm dia. illuminator focusing lens and the objective limited the minimum angle between the illuminator and the objective to about 35°. With 15° necessary to clear the specular reflection off the objective, the target had to be tilted about 10° from the normal to the objective. The second arrangement used a longer focal length lens for the illumination and added a small turning mirror just outside the aperture of the lens. This resulted in a symmetric configuration with the target surface normal to the objective axis.

The streak images were taken simultaneously with the near specular in the latter configuration. The only difference was the addition of a cylinder lens in the argon laser beam before combining it with the dye laser beam. This lens causes the argon laser to be focused to a line on the target which is then reimaged on to the entrance slit of the camera. This not only maximizes the throughput of laser light but creates a confocal arrangement limiting the collection of light to only that from the target line.

Depolarization of the diffuse component of the reflected light caused the polarizing beam splitter to be ineffective in separating the dye and argon beams to the frame and streak cameras respectively. The Coumarin-500 dye normally used runs broad band from about 480nm to 550nm overlapping the 514nm argon line, precluding spectral separation. For these experiments we therefore converted the laser to Rhodamine-590 which runs between about 570nm and 630nm thus allowing spectral splitting. The Rhodamine laser is narrower banded than the Coumarin giving noticeably more speckle in the images. On the other hand considerably more output energy is available because it can be pumped with the doubled Yag instead of the tripled.

Shuttering in the μDF is generally regarded for three different purposes, experimental fast gating, equipment protection and personnel laser safety. Laser safety issues are standard high power considerations, with the additional caveat that they not interfere with laser stability or timing. Equipment protection is accomplished with a standard electrically driven photographic shutter in front of every photocathode device. The purpose of these shutters is to protect photocathodes and microchannel plates from high level room light illumination or long term low level laser illumination during alignment. The experimental gates are themselves multi tiered. Temporal resolution of the frame camera is provided by the 1ns dye laser pulse, while the 20ns gate of intensifier tube rejects self lighting from the experiment. The streak tube provides its own temporal resolution; however, it has a poor rejection ratio requiring both a pockels cell and a fast mechanical shutter to prevent bleed through of the argon laser. In the streak spectrometer, in addition to the streak tube, the microchannel plate intensifier is also gated to prevent bleed through. The dispersion of the grating also provides considerable protection to the spectrometer tubes.

Accurate cross timing of the flyer drive laser was accomplished by driving both the pump and Q-switch triggers directly from the μDF timing system. To calibrate the cross timing a fast photodiode was placed at the experiment location to simultaneously record the arrival pulses through a bare pigtail and the 1ns dye laser illumination pulse which is the system timing reference. This is also used to calibrate the fast photomultiplier at the drive laser.

The timing calibration and synchronization was complicated by the jitter between the systems. Great care was taken to minimize the Q-switch jitter of both the flyer drive and the illumination lasers. However, the cavity build up jitter in both lasers resulted in a 5-10ns relative jitter. Although we could measure the timing to within 0.5ns we could not predict the experiments to better than ±5ns. As a result, experiments at times close to the laser beam impact on the flyer, were conducted by setting a fixed nominal delay, then doing several shots allowing the jitter to sample the temporal space.

Experiments

Experiments reported here were conducted in several week long sessions from May 1993 through March 1994. An experimental configuration or camera setup generally took a few hours to assemble and align. Once functional we were generally able to fire twelve to sixteen shots a day, including data archiving and film processing time.

Experimental parameters include a full drive laser energy of about 30mj, incident on the flyer. We also conducted half and quarter energy experiments. The flyers used were .25μm, 1μm and 4μm thick. The dye laser for the frame illuminations was typically run at about .5mj, at the laser. The laser was focused to a one millimeter spot on the target and neutral

density filters (typically ND 1-2) in the laser beam were used to adjust exposure. Polaroid Type 52 (ASA 400) was used to set exposures for the Kodak TMAX-400 data collection film. The extreme dynamic range of the TMAX film (linear nearly to density 4) makes it highly forgiving of experimental surprises and pulse to pulse illumination level changes. In some situations we push the film to ASA-1600, at which time Polaroid Type-57 is used for setup.

Initial experiments used only the frame camera in the first near specular configuration. These experiments revealed a complex pattern impressed on the flyer at jump off (Figure 4) The experiments did not, for the most part, damage the surface of the fiber pigtail from which the flyer had been launched. Consequently we were able to use a beam profiler to examine the laser beam at the fiber surface. The comparison of the profiler image with the dynamic image of the flyer surface suggested that the fiber optic transmission modes cause the patterning (Figure 5). A few 250μm diameter coated pigtails were available. However, the best matching taper had only a 200μm diameter. The results featured a low order mode caused by the improperly matched taper. Fewer, coarser higher order structures observed are consistent with fewer modes in a smaller fiber
(Figure 6).

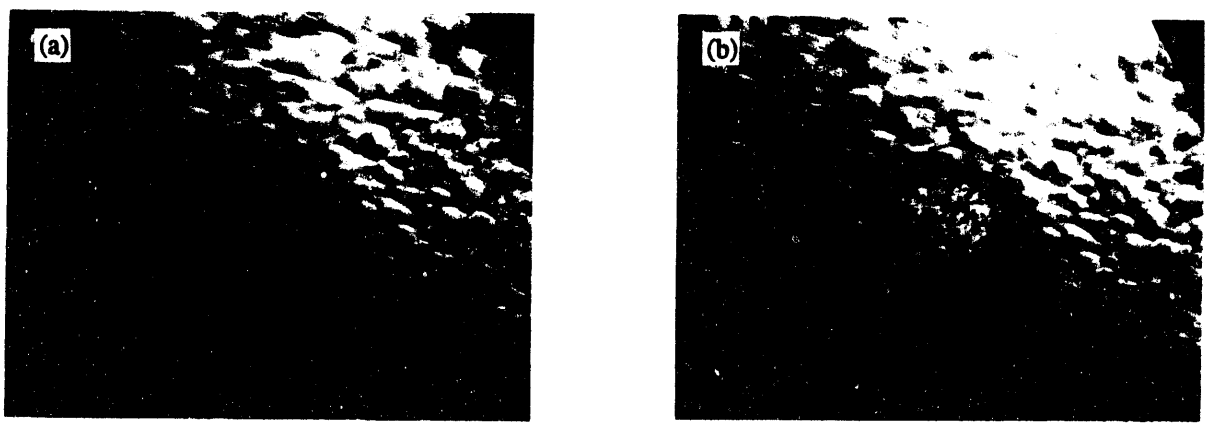

Preshot 20ns after laser peak.

Figure 4. Near specular images of laser launched flyer.

Note! In the preshot, the flyer is the smooth central region, the pockmarked region surrounding it is the ferule holding the fiber.

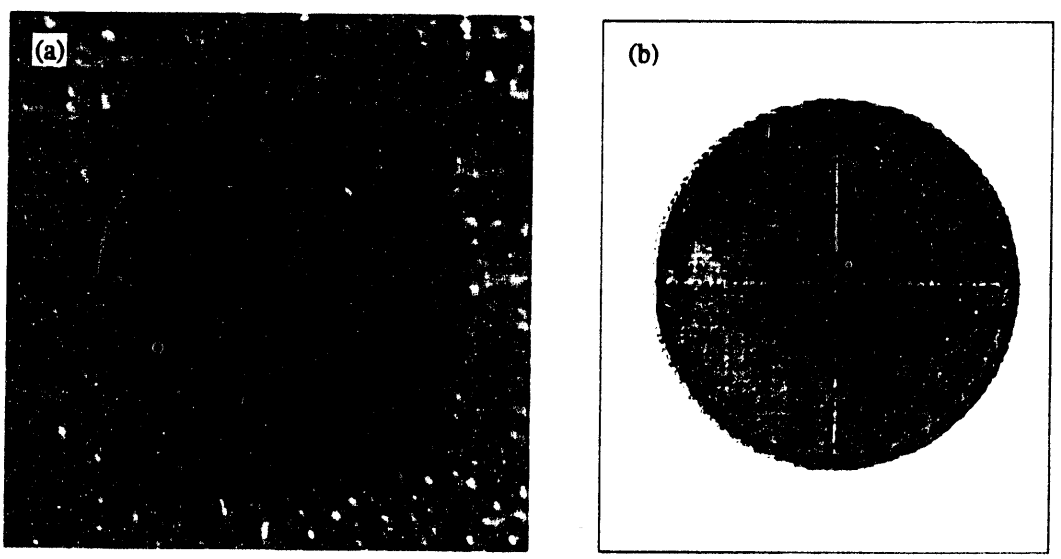

Figure 5. Comparison of a.)flyer surface at peak of laser pulse with b.)beam profile of subsequent laser pulse through same fiber pigtail.

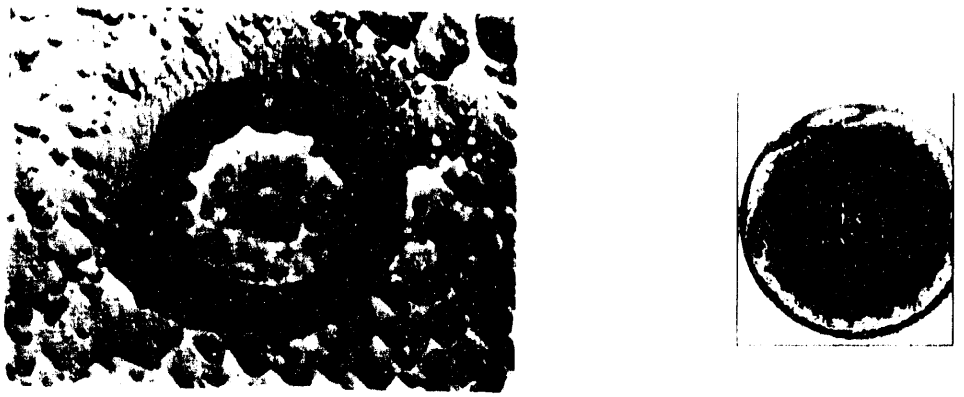

Figure 6. 250μm fiber/flyer a.)1ns before peak of laser pulse. b.)subsequent beam profile. The crack seen in the profile was not seen in the preshot.

Depth of focus and jitter precluded examining the flyers traveling towards the lens at more than a few nanoseconds after jump off. Also the reflective configuration gave no information as to the depth of the observed structures. We therefore switched to the shadowgraph mode with the flyer traveling perpendicular to the objective. The images (Figure 7) were predominated by the plasma absorption. The disturbance front was surprisingly flat. If one could believe that the perturbations in the front were just those of the flyer then they were not larger than about 8μm. Even more interesting is that once created they did not appear to grow in more than 50ns after jump off. This we interpreted as due to residual strength in the flyer.

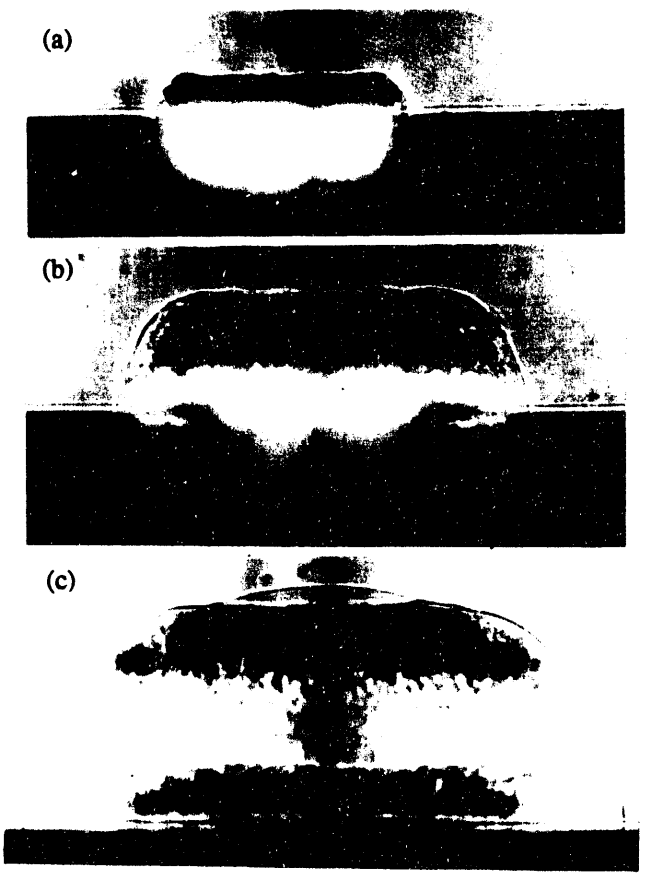

Figure 7. Shadowgraphs of flyer rising from bottom of image, at times after laser impact of; a.)30ns, b.)60ns, c.)120ns

The predominance of plasma effects especially in the later time images suggested adding the steak spectrometer. The spectrogram (Figure 8) shows a strong early time rapidly decaying continuum. A strong aluminum line appears with both broadened emission and absorption structures. Four highly broadened and as yet unidentified lines also are evident. The most surprising result was a late time flash. The flash was observed in all of the half dozen spectra recorded but its timing varied from about 80ns to over 120ns after jump off.

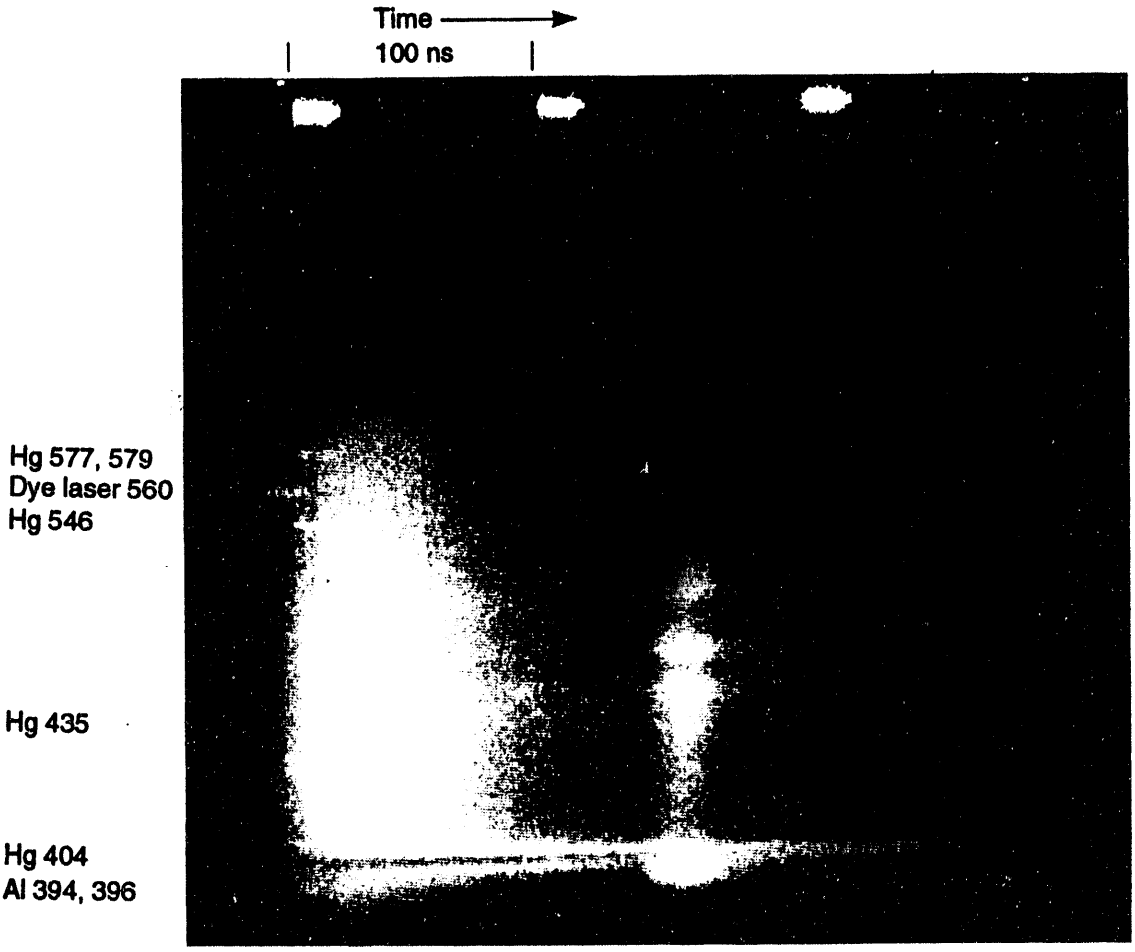

Figure 8. Streak spectrogram of plasma behind laser driven flyer. The dye laser pulse shows up at 560 nm indicating the relative time of the image. The mercury (Hg) lines are a calibration spectrum added before the shot. Temporal resolution is broadened to 15 ns by astigmatism of the spectrograph.

Returning to the second reflective configuration and adding the streak camera, we were able to record the entire vaporization process of a thin flyer (Figure 9). In the case of thin flyers, all the streak records showed the initial deformation of the flyer followed by a dramatic darkening or loss of reflectivity. This was rapidly followed by a strong, expanding, self luminosity. For thick flyers the initial deformation appears stable until the illumination is lost as the flyer moves out of the confocal region. A radially expanding luminosity is also observed outside the flyer area (Figure 10).

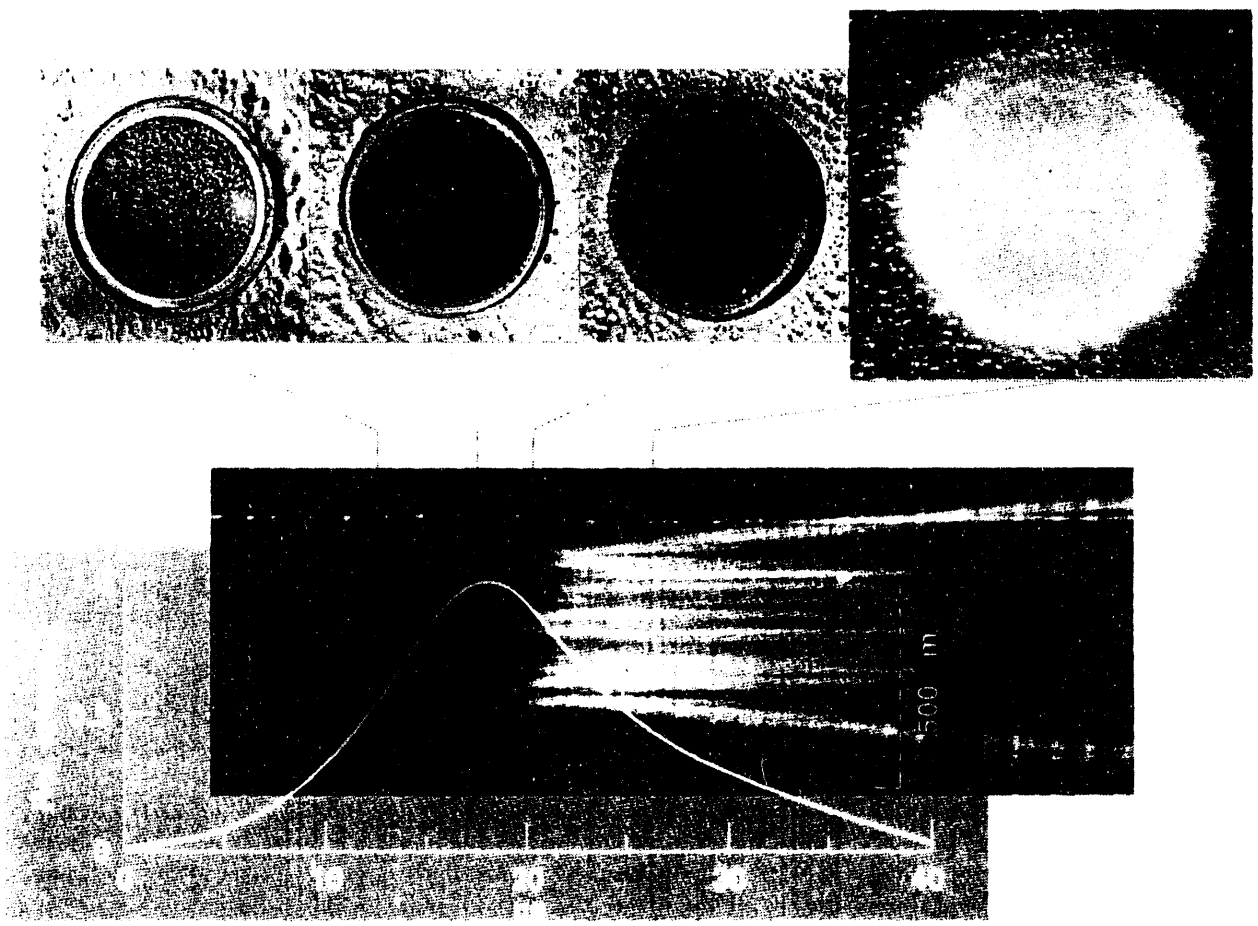

Figure 9. Response of a thin foil to high power laser impulse. The frame images from left to right show the initial deformation, vaporization then ionization of the foil. The curve superimposed on the streak record is the temporal profile of the drive laser pulse.

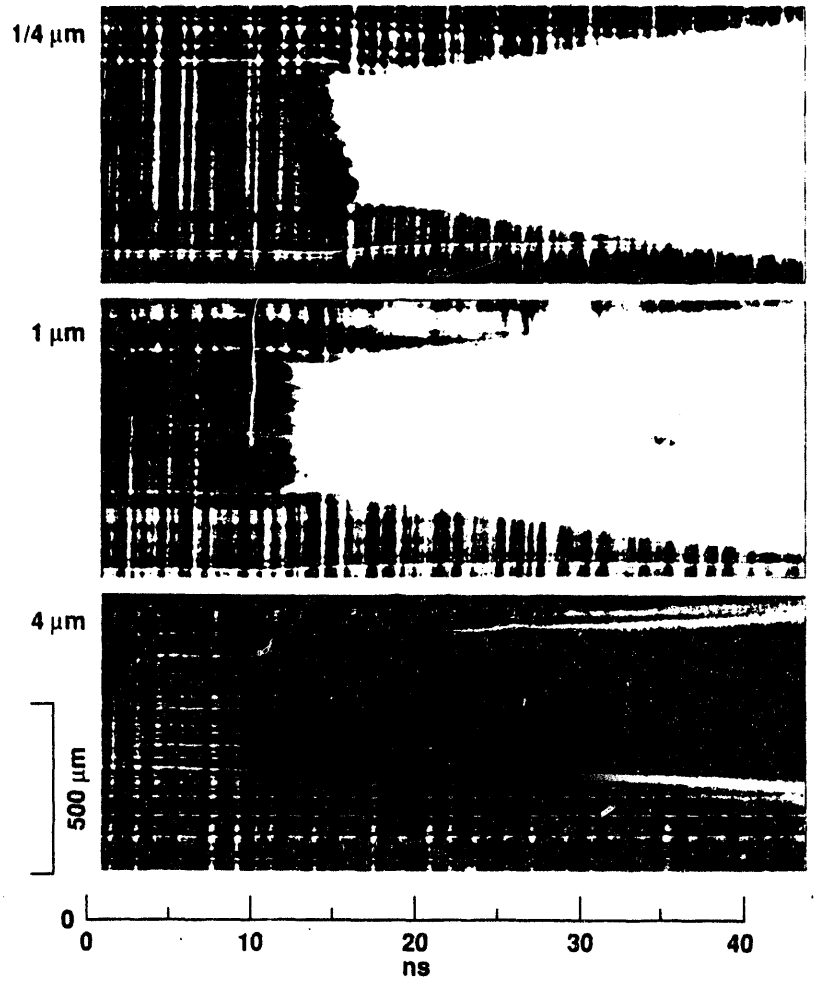

Figure 10. Streak records of the response of a.)0.25μm, b.)1μm and c.)4μm foils.

Capturing all the thin flyer phases on the frame camera was tricky, because the residual laser jitter was larger than the dark phase. Thus we had no a priori knowledge when the frame would occur. Consequently we could not adjust exposures for the very large brightness differences in each phase. Our solution was to expose for minimum useful exposure in the dark phase then develop the film normally. Relying on the dynamic range of the film and contrast modification in the printing process, we were able recover useful images from each phase. We are able to extract the exact timing relationships after the fact, from fiducial data on the film, digitizer and oscilloscope records. As crucial timing data was on the film we could not use that data to adjust our development process.

The frame images revealed structure carrying through the dark phase but the luminous phase is virtually structureless. In one image in the luminous region there appeared to be a spray of residual aluminum particles or droplets. However, this result could also be interpreted as grain clumping in the film emulsion. The image was extremely dense in that region of the negative and was printed at maximum contrast.

Comments

Our interpretation of the three phases is that an aluminum plasma is initially formed at the fiber / flyer (silica/aluminum) interface. As the flyer lifts off the silica, it is mechanically deformed by localized energy density perturbations caused by the fiber propagation modes. The deformation is arrested by the strength in the metal layer before much material is lost. Additional laser energy is absorbed by the plasma. The expanding plasma accelerates but also erodes the flyer. If there is sufficient energy, or the flyer is sufficiently thin, the front surface first vaporizes (dark phase) then ionizes (luminous phase). The front face of the thick flyer never vaporizes but is accelerated with the plasma expanding radially behind it. It is interesting that in over forty shots flyers either remained solid or appeared to transition to the ionized phase. None remained in the dark phase and there was only the hint of residual particles or droplets in the luminous phase.

At the present time we do not understand the late time plasma dynamics or the origin of the late flash. A late time pulse from the driver laser/fiber system was looked for, but not observed at energies down to 10^{-3} of the initial pulse. The stochastic timing of the flash tends to preclude an optical system effect. The shadowgraph images seem to indicate a backward propagating plasma that is larger than the flyer in diameter. It is possible that this plasma impacts the surface of the fiber ionizing more aluminum from the ferrule region creating the flash. We hope to revisit these issues in future experiments.

Acknowledgments

The authors wish to acknowledge the support of all those both at LLNL and SNLA who made this work possible. We would particularly like to recognize the continuing support
and useful technical input of Bob Setchell at Sandia and Ron Lee at Livermore.

Work supported by the U.S. Department of Energy at Sandia National Laboratories under contract DE-AC04-94-AL85000, and at Lawrence Livermore National Laboratory under contract W-7405-ENG48.

References

1. S.P. Obenschain, et al, Phys Rev. Let, 50:1, 3 Jan. '83, pp. 44-48.
2. P. Krehl, et al, JAP, 46:10, pp. 4400-4406, Oct. '75.
3. F. Cottet & J. P. Romain, Phys Rev. A, 25:1, pp. 576-579, Jan. '82.
4.L. R. Vesser. et al. APL 35:10. pp. 761-763, Nov. '79.
5. D. L. Paisley, Shock Compression of Condensed Matter-1989, S. C. Schmidt, et al, ed. Elsevier Sci. Pubs. B. V., 1990.

6. W. M. Trott & K. D. Meeks, Shock Compression of Condensed Matter-1989, S. C. Schmidt, et al, ed. pp. 997-1000, Elsevier Science, New York, 1990.

7. R. J. Lawrence & W. M.. Trott, Journal de Physique, Colloque C3, 453, 1991.
8. A. V. Farnsworth & R. J. Lawrence, Shock Compression of condensed Matter-1991, Schmidt, et al, ed. pp. 829-832, Elsevier Science, New York. 1992.

9. R. E. Setchell, et al, SPIE Proc. Symp. on Optical Materials for High Power Lasers, Boulder, Colorado, 1990.

10. L. L. Shaw, et al, 16th Congress on High Speed Photography, SPIE, Vol. 491, 1984.

11. A. M. Frank & D. F. Hein, 16th congress on High Speed Photography, SPIE, Vol. 491, 1984.
12. A. M. Frank, 18th Congress on High Speed Photography, SPIE, Vol. 1032, 1988.

DATE
FILMED
10/14/94
END